

Lymphotoxin- β regulates periderm differentiation during embryonic skin development

Chang-Yi Cui¹, Makoto Kunisada¹, Diana Esibizione^{1,2}, Sergei I. Grivennikov³, Yulan Piao¹, Sergei A. Nedospasov⁴ and David Schlessinger^{1,*}

¹Laboratory of Genetics, National Institute on Aging, National Institutes of Health, Baltimore, MD 21224, USA,

²Department of Histology, Embryology and Applied Biology, University of Bologna, Bologna 40126, Italy, ³Basic Research Laboratory, National Cancer Institute, PO Box B, Frederick, MD 21702, USA and ⁴Engelhardt Institute of Molecular Biology, Russian Academy of Sciences, Moscow 119991, Russia

Received May 03, 2007; Revised and Accepted July 24, 2007

Lymphotoxin- β (LT β) is a key regulator of immune system development, but also affects late stages in hair development. In addition, high expression of LT β at an early stage in epidermis hinted at a further function in hair follicle induction or epithelial development. We report that hair follicles were normally induced in LT β ^{-/-} skin, but the periderm detached from the epidermis earlier, accompanied by premature appearance of keratohyalin granules. Expression profiling revealed dramatic down-regulation of a gene cluster encoding periderm-specific keratin-associated protein 13 and four novel paralogs in LT β ^{-/-} skin prior to periderm detachment. Epidermal differentiation markers, including small proline-rich proteins, filaggrins and several keratins, were also affected, but transiently in LT β ^{-/-} skin at the time of abnormal periderm detachment. As expected, Tabby mice, which lack the *EDA* gene, the putative upstream regulator of LT β in skin, showed similar though milder periderm histopathology and alterations in gene expression. Overall, LT β shows a primary early function in periderm differentiation, with later transient effects on epidermal and hair follicle differentiation.

INTRODUCTION

The regulatory circuit for skin development must engineer transitions that start at embryonic day 13.5 (E13.5). At that time mouse skin epithelium consists of a single basal layer of undifferentiated keratinocyte progenitors with an overlying layer called the periderm (1). Committed basal keratinocytes then exit from cell cycle and start to differentiate to form stratified epidermis, and critical reciprocal interactions between epithelium and mesenchyme initiate skin appendage development at sharply defined times from E13.5 to E18.5 (2). During epidermal stratification, keratinizing keratinocytes in the upper epidermis express differentiation markers that include loricrin, involucrin, filaggrin and several keratins (3). They eventually form the characteristic structural features—cornified cell envelopes (CEs), keratohyalin granules and patterned keratins—that mark the terminal differentiation of skin (3).

The first stage in this process involves the little studied periderm, a transitory embryonic skin tissue consisting of a distinct cell population, that is, derived from basal keratinocytes about E8.5 (1). The periderm precursor cells detach from the basement membrane and migrate to the skin surface to form a single layer 'cell-net' (1). The periderm cells are connected by tight junctions, which are conspicuously lacking in the underlying epidermis during stratification. The periderm communicates closely with the epidermis, and it is thought to stabilize both differentiating epidermis and epithelium–mesenchyme interactions (1,4). Accordingly, periderm removal during epithelium–mesenchyme interaction for limb development results in ventral polydactyly in rats (5). Once epidermal stratification is complete at E18.5, the periderm is apparently superannuated and is shed from the underlying epidermis. However, the molecular mechanism of periderm differentiation and function in skin development is poorly understood (6).

*To whom correspondence should be addressed at: Laboratory of Genetics, National Institute on Aging/NIH 333 Cassell Dr., Suite 3000, Baltimore, MD 21224, USA. Tel: +1 4105588337; Fax: +1 4105588331; E-mail: schlessingerd@grc.nia.nih.gov

Here we report that lymphotoxin- β (LT β), a member of the TNF ligand superfamily that is a well known immunomodulatory cytokine, also involved in regulating lipid metabolism (7,8), has a pivotal role in periderm homeostasis. LT β expression in skin epithelium peaked at E14.5 and was thereafter confined to hair follicles at a lower level (9). We previously showed that its late action in hair follicles regulate hair shaft formation (9). We now report that the earlier expression of LT β in skin epithelium regulates periderm differentiation, at least in part through periderm-specific keratin-associated proteins (KAPs), and subsequently transiently affects epidermal differentiation.

RESULTS

Normal induction of hair follicles, but abnormal differentiation of periderm and epidermis in LT $\beta^{-/-}$ mice

Because LT $\beta^{-/-}$, but not LT $\alpha^{-/-}$ or LT $\beta R^{-/-}$ mice showed striking hair phenotypes, we looked more extensively for a possible action of LT β in skin (9). The strong expression of LT β in early stage embryonic skin suggested two possible roles: (1) LT β regulates epithelium development at early stages and hair follicle differentiation at late stages or (2) LT β regulates hair follicle induction as well as hair follicle differentiation from an early stage, with no pronounced effect on epithelium. To distinguish between these alternatives, we collected wild-type and homozygous LT $\beta^{-/-}$ embryos at E14.5, 15.5, 16.5 and 18.5, and initially carried out morphological analyses. No gross defects were seen in mutant embryos as compared to wild-type controls at any developmental time point (Supplementary Material, Table S1a). By histological analyses, we observed normal induction of hair germs at E14.5 in LT $\beta^{-/-}$ skin (Fig. 1A, solid lines at E14.5) and normal down-growth from E15.5 onward (Fig. 1A, arrows at E15.5 and arrowheads in E16.5). These results argue against any early effect of LT β on hair follicles.

To test the alternative of an effect on early epithelium development, we analyzed skin epithelium more closely and found striking histological abnormalities in the periderm in LT $\beta^{-/-}$ mice. The periderm normally covers the epidermis from E8.5 until E17.5 and disappears thereafter (6). Thus, we found that the periderm was intact until E16.5 in wild-type skin (Fig. 1B, depicted by broken lines) and then starts to detach. In contrast, in LT $\beta^{-/-}$ mice the periderm was almost completely detached from underlying epidermis at E16.5, one or two days earlier than in wild-type mice (Fig. 1B, arrowheads in E16.5). By immunofluorescent staining with a periderm marker, keratin 6a (10), we further confirmed that periderm was intact until E16.5, but largely detached at E18.5 in wild-type embryos (Fig. 1C; arrows indicate remnants of periderm). In contrast, periderm was lost by E16.5 in LT $\beta^{-/-}$ embryos (Fig. 1C).

In addition, at E16.5, epidermal differentiation was also altered in mutant mice. Keratohyalin granules appeared precociously in the upper epidermis, and some embryos even started to form stratum corneum (Fig. 1B, E16.5, arrows in the insert indicate premature appearance of keratohyalin granules and overlying pink horny layer in LT $\beta^{-/-}$ mice). By E18.5, keratohyalin granules were also formed in wild-type embryos (Fig. 1B, E18.5).

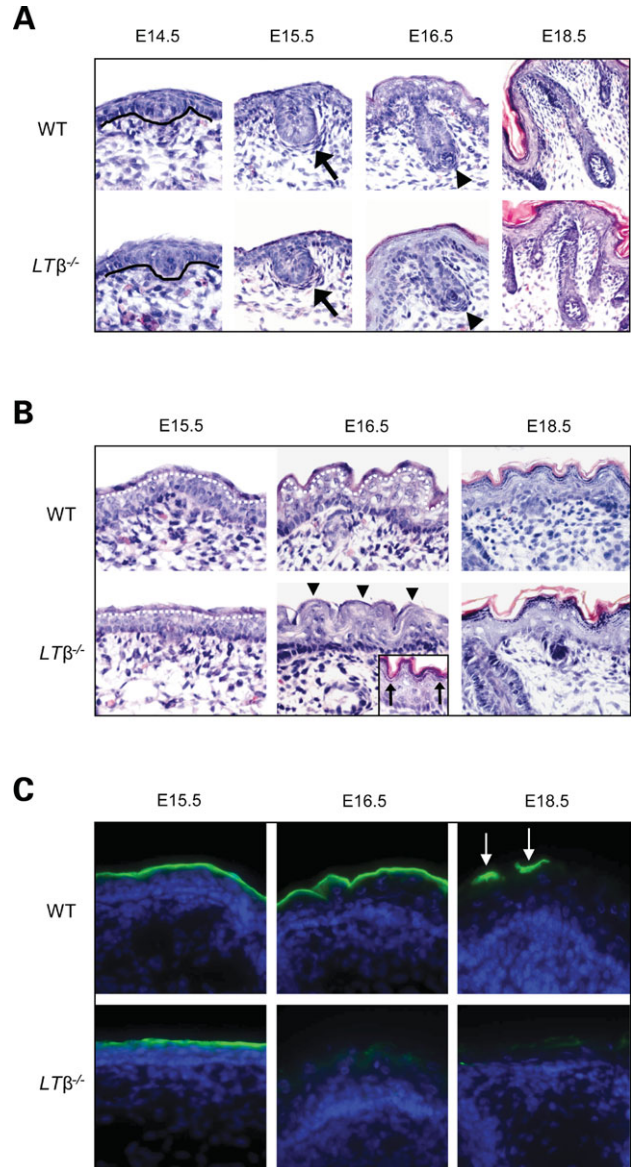


Figure 1. Histology of LT $\beta^{-/-}$ embryonic skin at successive time points. (A) Hair germs were normally initiated at E14.5 (demarcated by solid line), and were normally growing from E15.5 onward (arrows) in LT $\beta^{-/-}$ mice compared to wild-type. Dermal papillae were normally forming at E16.5 (arrowheads), and hair shafts were made at E18.5 both in wild-type and LT $\beta^{-/-}$ embryos. (B) Periderm (depicted by broken lines) was nearly normal in LT $\beta^{-/-}$ embryos at E15.5, but was almost completely detached at E16.5 (arrowheads). Some embryos developed keratohyalin granules (arrows in insert) and overlying pink stratum corneum at E16.5 in LT $\beta^{-/-}$ embryos. Keratohyalin granules appeared in both wild-type and LT $\beta^{-/-}$ skin at E18.5, but were more pronounced in mutant skin. (C) Immunofluorescent staining with an antibody against Keratin 6a (green) revealed that in wild-type embryos the periderm was normal until E16.5 and mostly detached at E18.5 (arrows indicate remnants of periderm). In contrast, the periderm was gone by E16.5 in LT $\beta^{-/-}$ embryos.

The apparent anomalies in differentiation of skin epidermis led us to investigate possibly affected differentiation markers in further detail. We performed immunofluorescent staining with antibodies against major epidermal differentiation markers including filaggrin, loricrin, keratin 1 and keratin 14 (Fig. 2 and Supplementary Material, Table S1b). Other

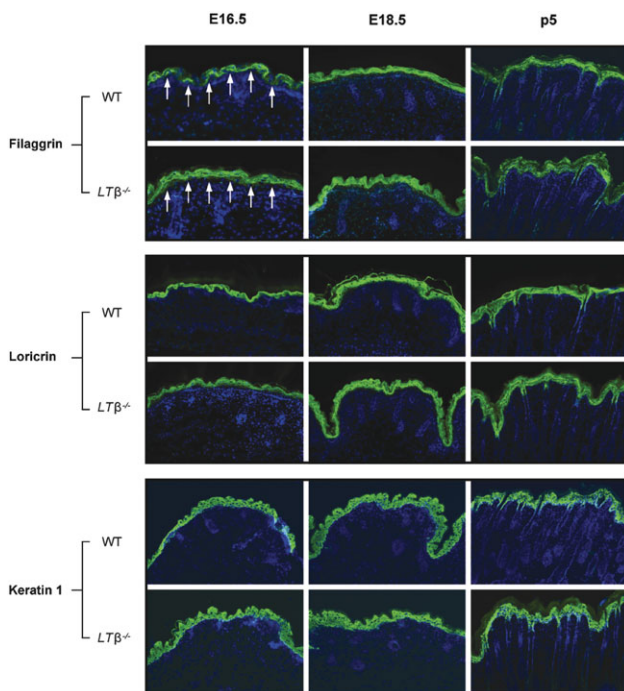


Figure 2. Immunofluorescent staining for epidermal differentiation markers at successive time. Filaggrin was significantly upregulated in $LT\beta^{-/-}$ skin at E16.5 (arrows in upper left panels), and slightly at E18.5 and p5. No significant expression differences were found between wild-type and $LT\beta^{-/-}$ skin for loricrin or keratin 1.

markers were not affected in $LT\beta^{-/-}$ skin, but the expression of filaggrin, the major component of keratohyalin granules, was significantly elevated at E16.5, staining strongly from the middle squamous layer to the horny layer (Fig. 2, arrows in upper left panels). Elevation of filaggrin was stage specific: it had not yet begun at E15.5, peaked at E16.5, and was still seen at E18.5 and in newborn mutant mice, though not as abundantly as at E16.5 (Fig. 2).

The aberrant differentiation of periderm and underlying epidermis in $LT\beta^{-/-}$ embryos was thus in contrast to the apparent normal induction of hair follicles.

Marked downregulation of periderm specific KAP genes in $LT\beta^{-/-}$ mice

To look for the spectrum of genes affected in $LT\beta^{-/-}$ skin, we carried out whole genome microarray expression analyses with skin samples from wild-type and mutant embryos. Based on the most evident histological abnormalities at E16.5, we have chosen four time points, E15.5, E16.5, E18.5 and postnatal day 5 (p5) for expression profiling (Supplementary Material, Table S1a).

Striking changes in expression were found for several periderm-specific genes. *KAP13* and three novel *KAP13*-like genes, *2310034C09Rik*, *LOC546672* and *LOC433047* were dramatically down regulated in $LT\beta^{-/-}$ skin 10-fold at E15.5 and >100-fold at E16.5, i.e. both before and after premature periderm detachment (Fig. 3A). Another paralogous gene, *2310057N15Rik*, was weakly expressed in wild-type and mutant skin at E15.5, but significantly upregulated only

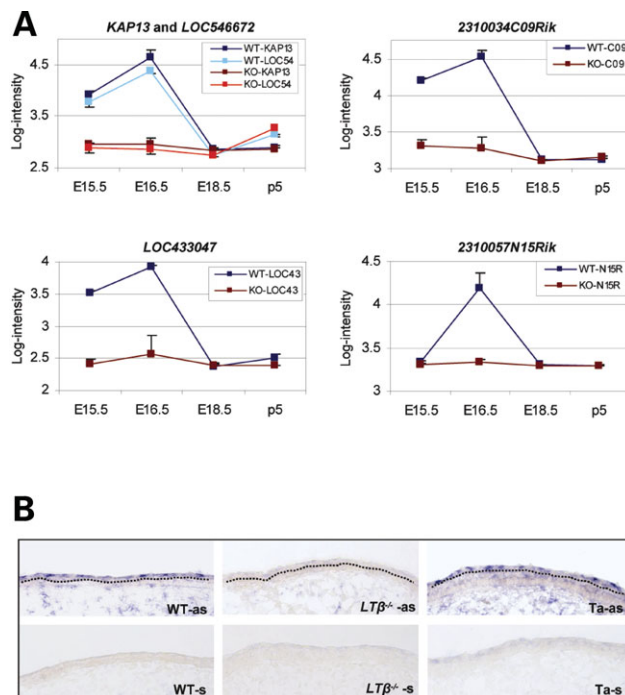


Figure 3. Expression of *KAP13* and its paralogous genes in wild-type and $LT\beta^{-/-}$ skin. (A) Expression levels from microarray assays, shown as log-intensities. Expression of *KAP13*, *LOC546672*, *2310034C09Rik*, *LOC433047* was high at E15.5 and E16.5 in wild-type skin but sharply down regulated in $LT\beta^{-/-}$ skin. In contrast, expression of another paralog, *2310057N15Rik*, was low at E15.5, but sharply upregulated at E16.5 in wild-type skin (right lower panel). At E18.5 and p5, expression of all five genes was at basal levels both in wild-type and $LT\beta^{-/-}$ skin. (B) *In situ* hybridization assays revealed specific localization of *KAP13* transcripts in the periderm of wild-type and Tabby skin, but not in $LT\beta^{-/-}$ at E15.5 (upper panels). No signals were found from sense probes (lower panels). as, anti-sense, and s, sense probes.

in wild-type at E16.5 (Fig. 3A, bottom right panel). Notably, from E18.5 onward, all five genes were expressed at background levels even in wild-type mice, and expression differences between wild-type and $LT\beta^{-/-}$ skin were no longer evident (Fig. 3A). This is consistent with the programmed detachment of the periderm, harboring these protein components, during the differentiation process. The time course of expression and loss was almost identical for *KAP13*, *2310034C09Rik*, *LOC546672* and *LOC433047* in wild-type and mutant skin (Fig. 3A). To verify these findings by an independent method, we carried out Taqman real-time PCR assays for *KAP13*, *2310034C09Rik* and *2310057N15Rik*. Compared with microarrays, real-time PCR assays showed even greater expression differences between wild-type and $LT\beta^{-/-}$ skin (Supplementary Material, Table S2). *In situ* hybridization assays further confirmed the *KAP13* transcripts in the periderm of wild-type and Tabby skin at E15.5; which was undetectable in $LT\beta^{-/-}$ skin (Fig. 3B, upper panels).

The five genes, especially *KAP13*, *2310034C09Rik*, *LOC546672*, and *2310057N15Rik*, encode highly homologous proteins (Fig. 4A). The periderm genes are tightly clustered within 60 kb of DNA in the 'KAP complex' on mouse chromosome 16 C3.3. No additional genes in this region are evident in the current genomic DNA assemblies, where they

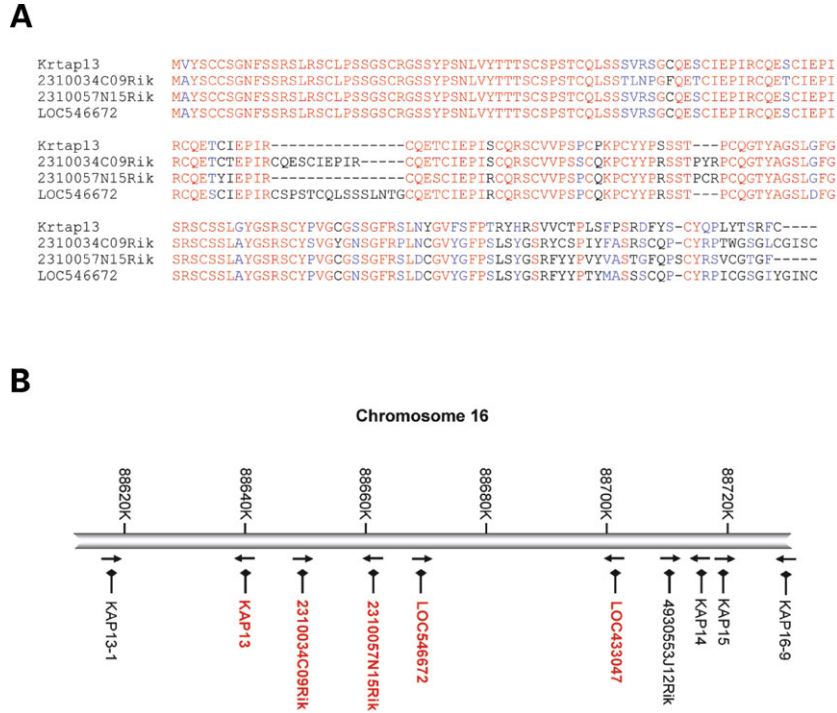


Figure 4. Protein homology and clustering of *KAP13* paralogue genes on mouse chromosome 16. (A) Protein homology between *KAP13*, 2310034C09Rik, 2310057N15Rik, and LOC546672. Red, identical; blue, similar amino acids. (B) *KAP13* and 4 paralogue genes (red) were tightly clustered within 60 kb distance of the ‘*KAP* locus’ on chromosome 16, C3.3. Arrows indicate transcription direction for each gene.

are transcribed in different directions in a pattern that suggests the presence of multiple promoters (Fig. 4B).

In contrast to *KAP13* and its paralogue genes, keratin 6a (*Krt6a*), another gene specific to periderm (10), was sharply downregulated in *LTβ*-deficient skin at E16.5, the time of premature periderm detachment, by microarray expression profiling and real-time PCR assays (Supplementary Material, Table S3a), consistent with immunofluorescent staining (Fig. 1C). Whether *KAP13* paralogs interact with *Krt6a* for periderm differentiation is unknown.

Transiently affected epidermal differentiation markers at E16.5 in *LTβ*^{-/-} skin

Terminal differentiation of skin epidermis is marked by formation of three characteristic structures: the cornified CEs, consisting of loricrin, involucrin, small proline-rich proteins (Sprrs), repetin, etc.; the keratohyalin granules mainly comprised of profilaggrin, the precursor of filaggrin and the patterned keratins occurring in bundles (3). These components contribute to the formation of the epidermal barrier and highly insoluble, mechanically tough corneocytes (11). At the time of premature periderm detachment in mutant skin, we found significant expression changes for components of the cornified CEs and keratohyalin granules, encoded by a cluster of genes in the ‘epidermal differentiation complex’ locus on chromosome 3 F1-2.

At E15.5, only two differentiation related genes, the Sprr-like 2310002A05Rik, and 2300002G24Rik, encoding a novel cysteine-rich protein, were significantly downregulated in mutant skin (Table 1, E15.5). By E16.5, the number of

Table 1. Genes from the epidermal differentiation complex affected in *LTβ*^{-/-} skin

Genes	Fold-differences (<i>LTβ</i> ^{-/-} / WT)				Chr.3	Strand
	E15.5	E16.5	E18.5	p5		
<i>Sprr2a</i>	0.98	1.89	1.14	1.02	F1	(+)
<i>Sprr2d</i>	1.05	5.20	2.17	1.24	F1	(+)
<i>Sprr2h</i>	1.06	1.93	0.85	0.93	F1	(+)
<i>Rptn</i>	0.94	2.24	0.72	1.22	F2	(+)
<i>Sprr1b</i>	1.26	<i>0.47</i>	1.22	1.56	F1	(-)
<i>Sprr1a</i>	0.75	<i>0.32</i>	1.03	1.09	F1	(-)
2310002A05Rik ^a	<i>0.54</i>	<i>0.04</i>	1.19	1.07	F1	(+)
2300002G24Rik	<i>0.46</i>	1.21	1.26	1.02	F2	(-)
<i>Flg2</i>	1.04	3.47	0.95	0.97	F2	(+)
<i>Flg</i>	0.98	3.70	1.07	1.04	F2	(+)

Bold-face, upregulated; italics, downregulated in *LTβ* mutant skin. ^aSprr-like, ‘late cornified envelop protein’.

genes affected had grown to 9 (Table 1, E16.5). *Sprr1a*, *1b* and Sprr-like 2310002A05Rik were sharply downregulated in mutant skin, and in contrast, *Sprr2a*, *2d*, *2h* and *repetin* were significantly upregulated. Downregulation of *Sprr1a* protein in mutant skin was confirmed by immunofluorescent staining (Supplementary Material, Table S3b). Sprr proteins are coexpressed with loricrin in cornified CEs and serve as cross-linkers (12); and upregulation of *Sprr2d*, *2h* and *repetin* was previously reported in loricrin-deficient mice (13). Surprisingly, at E18.5 and p5, the expression of these components in mutant skin had reverted to normal level (Table 1, E18.5 and p5). This suggested that a compensatory

Table 2. Keratin genes affected in *LTβ*-deficient skin (*LTβ*^{-/-}/WT)

Genes	E15.5	E16.5	E18.5	p5	Chr.	Strand
<i>Krt12</i>	1.04	2.78	1.32	1.00	11D	(-)
<i>Krt16</i>	0.99	1.56	1.28	1.04	11D	(-)
<i>K27</i>	1.09	2.27	1.18	1.00	11D	(-)
<i>K71</i>	1.03	1.59	1.27	1.04	15F2	(-)
<i>Krt6a</i>	1.09	<i>0.22</i>	1.12	0.78	15F2	(-)
<i>Krt19</i>	0.94	<i>0.25</i>	0.90	0.78	11D	(-)
<i>Krt4</i>	1.01	<i>0.39</i>	0.95	1.00	15F3	(-)
<i>Krt7</i>	1.20	<i>0.5</i>	0.81	0.98	15F2	(+)
<i>Krt8</i>	0.79	<i>0.53</i>	0.88	0.98	15F3	(-)
<i>Krt13</i>	1.10	<i>0.65</i>	1.08	0.93	11D	(-)
<i>Krt18</i>	0.78	<i>0.56</i>	0.86	0.93	15F3	(+)
<i>Krt23</i>	<i>0.67</i>	1.25	0.94	0.93	11D	(-)

Bold-face and italics indicate up and downregulated genes in *LTβ*-deficient skin, respectively. Genes in upper part are hair follicle related genes.

mechanism may exist, as already indicated for loricrin and involucrin-deficient mice (13,14). Transcription of the major cornified CE components, such as loricrin and involucrin (15), however, remained unchanged in mutant mice.

In addition, we found that expression of filaggrin and its paralog filaggrin 2, the major components of keratohyalin granules, was significantly upregulated in mutant skin at E16.5 (Table 1), consistent with protein expression assessed by immunofluorescent staining (Fig. 2). No change in transcription of filaggrin was detected at E18.5 and p5 (Table 1), but immunostaining showed slightly upregulated protein expression in mutant skin at those times (Fig. 2).

Further striking changes were found in the expression of 12 keratin genes, half of them known to be hair follicle related (Table 2). For example, *Krt27* is specifically expressed in inner root sheath (IRS) and medulla of hair follicles (16), and *Krt71* mutations affect IRS and hair shaft formation (17). Both genes were significantly upregulated in *LTβ*^{-/-} skin (Table 2, E16.5). Real-time PCR assays with probe/primers for *Krt71* corroborated these microarray results (not shown). Altered expression of these genes may contribute to the abnormal hair shaft formation observed in *LTβ*^{-/-} mice (9). However, like most of the 'epidermal differentiation complex' genes, their transcription was affected only at E16.5. Other major epidermal keratins *Krt1*, 5, 10 and 14 were not affected in mutant skin.

Similar but milder periderm phenotypes and delayed expression changes for *KAP* genes in *EDA* mutant Tabby mice

We have reported that *LTβ* to be a potential target of *EDA* signaling (9). If *LTβ* is tightly regulated by *EDA* in periderm, similar periderm abnormalities can be expected from *EDA* mutant Tabby mice. We therefore analyzed back skin of Tabby mice before and during periderm detachment. Histology showed that periderm was intact at E15.5, but started to detach at E16.5 in Tabby hemizygous and homozygous mice, when it was still firmly attached in control wild-type and heterozygous Tabby females (Fig. 5A). These findings agree with earlier observations by Vielkind and Hardy (18)

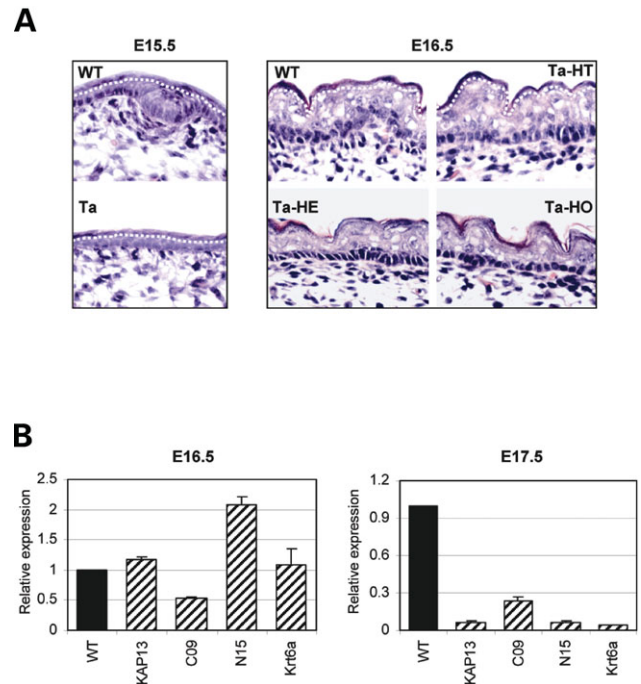


Figure 5. Histology of periderm and expression levels of periderm-specific genes in *EDA* mutant Tabby skin. (A) Periderm was normal in Tabby (Ta) at E15.5. At E16.5, periderm was still intact in wild-type and heterozygous Tabby (Ta-HT) females, but was detaching from hemizygous (Ta-HE) and homozygous (Ta-HO) Tabby littermates. Broken lines demarcate periderm. (B) Only *2310034C09Rik* (C09) was downregulated in Tabby at E16.5, but all four genes were sharply downregulated at E17.5.

and similar to observations in *LTβ*^{-/-} mice (Fig. 1B). However, the periderm phenotype in Tabby is milder and delayed compared with that in *LTβ*^{-/-} mice. For instance, at E16.5, only some parts of periderm were detached in Tabby, whereas detachment was almost complete in *LTβ*^{-/-} mice (Figs 1B and C and 5A). By E18.5, the periderm was gone in both Tabby and wild-type mice (data not shown).

We carried out additional real-time PCR assays for *KAP13*, *2310034C09Rik*, *2310057N15Rik* and *Krt6a*, the genes most affected in *LTβ*^{-/-} mice at E16.5, using skin samples from littermate wild-type and Tabby embryos. At E16.5, in Tabby skin, expression of *KAP13* and *Krt6a* was comparable to wild-type controls, *2310057N15Rik* was higher, and *2310034C09Rik* was downregulated (Fig. 5B, left panel). However, at E17.5, expression of all four genes was sharply downregulated in Tabby (Fig. 5B, right panel), about 1 day later than *LTβ*^{-/-} mice but still sooner than in wild-type. The delayed expression changes in Tabby skin were consistent with histological findings (Fig. 5A).

Expression profiling revealed different downstream targets of *LTβ* in skin and in immune system

Based on the phenotypes of adult *LTβ*^{-/-}, *LTα*^{-/-} and *LTβR*^{-/-} mice, we previously suggested that *LTβ* may initiate a specialized signaling cascade in skin (9). To assess this possibility, we directly compared transcription profiles of *LTβ*^{-/-} skin and lymph nodes from animals with a lesion of *LTβ* limited to B-cells. Unlike mice with complete

(9,23–25). Unlike wide-spread *EDA* expression in skin epidermis and hair follicles, its receptor, EDAR, and receptor adaptor protein, EDARADD, are restricted to hair follicles from E14.5 onward. *EDA* signaling is therefore often thought to be inactive in skin epidermis and periderm (26–28). However, the periderm abnormalities in Tabby skin suggest that ectodysplasin functions there (Fig. 5A, reviewed in 18). We infer that either EDAR is weakly expressed or ectodysplasin has an indirect partner in skin epithelium.

Compared with *LTβ*-deficient mice, the periderm phenotype in Tabby mice was histologically similar, though milder and delayed. Expression changes of *KAP* genes in Tabby skin were also delayed and less extreme than in *LTβ*-deficient mice. In our previous study, the hair phenotype in *LTβ*-deficient mice was also milder than in Tabby; and sweat glands were normally developed in *LTβ*-deficient mice, but absent in Tabby. Furthermore, among a dozen epidermal differentiation markers affected in *LTβ*-deficient mice, only a minority, including *Sprr1a*, *Krt12* and *Krt7*, was transiently affected in Tabby (9). These data are consistent with findings that *EDA* signaling operates through multiple pathways (9), and there may be synergistic or compensating interactions of target pathways.

Also, unlike the case in the immune system, *LTα* and *LTβR* showed actions distinct from *LTβ* in skin (9). This reflects the involvement of a special *LTβ* receptor or interacting protein in skin or the presence of different downstream repertoires of signaling pathways in different tissues. Thus animal models have uncovered *LTβ* function in skin and lymphoid tissues, but with lesions in *LTβ* have not been reported (31). Nevertheless, *LTβ* has been shown to be involved in chronic inflammatory disease, and could conceivably affect periderm and hair follicles in humans as well (31).

MATERIALS AND METHODS

Timed-mating with mutant mouse strains

Two mutant mouse strains in C57BL6 background were used, *LTβ* knockout and *EDA* mutant Tabby mice. Two timed matings were set up separately to yield homozygous *LTβ* knockout, and Tabby hemizygous or homozygous embryos. Male and female *LTβ*^{-/-} mice were crossed to get *LTβ*^{-/-} embryos; and Tabby hemizygous mice were crossed with Tabby heterozygous mice to obtain wild-type and Ta hemizygous/homozygous embryos (C57BL/6J-A^{W-J}-Ta^{6J}, Jackson Laboratory). The morning after mating was designated as E0.5. Embryos were harvested at E14.5–E18.5. Back skin samples and livers were collected under a dissection microscope, frozen on dry ice and stored at -80°C until use. Genotyping was done as previously reported (9).

Embryo collection, RNA isolation, microarray assay and real-time PCR

RNAs from back skin samples of wild-type and *LTβ*^{-/-} embryos at E15.5, E16.5, E18.5 and p5 were profiled on microarrays. RNAs were isolated with Trizol (Invitrogen), LiCl precipitated, and their quality checked by electrophoresis, as previously reported (29). RNAs from three biological

replicates (from three different embryos) were hybridized to 44 000 feature 60-mer-oligo microarrays (30). Triplicate data were analyzed, with FDR set to ≤0.1, and genes with <1.5-fold difference were excluded from significant gene lists. We selected 10 genes, including *KAP13*, *2310034C09*, *2310057N15*, *Zfp318*, *Entpd4*, *Wdfy1*, *BC020077*, *Krt6a*, *Krt71* and *CCL19* for one-step real-time PCR confirmation with Taqman 'Assays on-Demand' probe/primers (Applied Biosystems).

In addition, we isolated RNAs from skin samples of Tabby and wild-type littermates at E16.5 and E17.5 for real-time PCR analyses by the methods described above.

Histology, immunofluorescent staining and *in situ* hybridization

For histological analyses, skin samples from back skin of strains each time point were fixed in 4% paraformaldehyde, embedded in paraffin, and 5 μm sections stained with hematoxylin/eosin. For immunofluorescent staining, anti-mouse keratin 6a (1:500 dilution, Covance), filaggrin (1:750, Covance), loricrin (1:250, Covance), *Krt14* (1:50, Santa Cruz Biotechnology) and *Krt1* (1:500, Abcam) antibodies were incubated with 10 μm frozen back skin sections, followed by Alexa-fluor secondary antibodies (Invitrogen), and were analyzed under a DeltaVision confocal microscope. For *in situ* hybridization, 14 μm frozen back skin sections were fixed in 4% paraformaldehyde and hybridized with a *KAP13*-specific cRNA probe overnight at 60°C. A full-length (902 bp) *KAP13* cDNA clone was purchased from Invitrogen and its sequence fully verified before synthesis of a cRNA probe. Digoxigenin (DIG)-labeled sense and antisense probes were prepared using a DIG RNA labeling kit (Roche). After washing with 2x SSC (0.3 M NaCl and 0.03 M sodium citrate, pH 7.0) and 0.1x SSC at 60°C, sections were incubated with anti-DIG antibody for 2 h and signals were visualized with NBT/BCIP stain (Biochain, 1:1000 dilution).

ACKNOWLEDGEMENTS

We thank Drs M. Ko and R. Nagaraja for helpful discussions and technical advices; E. Douglass, A. Butler and D. Nines for animal management. S.A.N. is International Research Scholar of Howard Hughes Medical Institute. This work was supported by the IRP of the National Institutes of Health, National Institute on Aging.

Conflict of Interest statement. None declared.

REFERENCES

1. M'Boneko, V. and Merker, H.J. (1988) Development and morphology of the periderm of mouse embryos (days 9–12 of gestation). *Acta Anat (Basel)*, **133**, 325–336.
2. Fuchs, E. (2007) Scratching the surface of skin development. *Nature*, **445**, 834–842.
3. Candi, E., Schmidt, R. and Melino, G. (2005) The cornified envelope: a model of cell death in the skin. *Nat. Rev. Mol. Cell Biol.*, **6**, 328–340.
4. Armstrong, M.T., Turlo, K., Elges, C.J., Dayton, S.M., Lee, J. and Armstrong, P.B. (2006) A novel form of epithelial wound healing of the embryonic epidermis. *Exp. Cell Res.*, **312**, 2415–2423.

5. Scott, W.J., Jr., Nau, H., Wittfoht, W. and Merker, H.J. (1987) Ventral duplication of the autopod: chemical induction by methoxyacetic acid in rat embryos. *Development*, **99**, 127–136.
6. Takaishi, M., Takata, Y., Kuroki, T. and Huh, N. (1998) Isolation and characterization of a putative keratin-associated protein gene expressed in embryonic skin of mice. *J. Invest. Dermatol.*, **111**, 128–132.
7. Tumanov, A.V., Kuprash, D.V. and Nedospasov, S.A. (2003) The role of lymphotoxin in development and maintenance of secondary lymphoid tissues. *Cytokine Growth Factor Rev.*, **14**, 275–288.
8. Lo, J.C., Wang, Y., Tumanov, A.V., Bamji, M., Yao, Z., Reardon, C.A., Getz, G.S. and Fu, Y.X. (2007) Lymphotoxin beta receptor-dependent control of lipid homeostasis. *Science*, **316**, 285–288.
9. Cui, C.Y., Hashimoto, T., Grivennikov, S.I., Piao, Y., Nedospasov, S.A. and Schlessinger, D. (2006) Ectodysplasin regulates the lymphotoxin-beta pathway for hair differentiation. *Proc. Natl. Acad. Sci. USA*, **103**, 9142–9147.
10. Mazzalupo, S. and Coulombe, P.A. (2001) A reporter transgene based on a human keratin 6 gene promoter is specifically expressed in the periderm of mouse embryos. *Mech. Dev.*, **100**, 65–69.
11. Segre, J. (2003) Complex redundancy to build a simple epidermal permeability barrier. *Curr. Opin. Cell Biol.*, **15**, 776–782.
12. Steinert, P.M., Candi, E., Kartasova, T. and Marekov, L. (1998) Small proline-rich proteins are cross-bridging proteins in the cornified cell envelopes of stratified squamous epithelia. *J. Struct. Biol.*, **122**, 76–85.
13. Koch, P.J., de Viragh, P.A., Scharer, E., Bundman, D., Longley, M.A., Bickenbach, J., Kawachi, Y., Suga, Y., Zhou, Z., Huber, M. *et al.* (2000) Lessons from loricrin-deficient mice: compensatory mechanisms maintaining skin barrier function in the absence of a major cornified envelope protein. *J. Cell Biol.*, **151**, 389–400.
14. Djian, P., Easley, K. and Green, H. (2000) Targeted ablation of the murine involucrin gene. *J. Cell Biol.*, **151**, 381–388.
15. Steven, A.C. and Steinert, P.M. (1994) Protein composition of cornified cell envelopes of epidermal keratinocytes. *J. Cell Sci.*, **107**, 693–700.
16. Langbein, L., Rogers, M.A., Praetzel-Wunder, S., Helmke, B., Schirmacher, P. and Schweizer, J. (2006) K25 (k25irs1), k26 (k25irs2), k27 (k25irs3), and k28 (k25irs4) represent the type I inner root sheath keratins of the human hair follicle. *J. Invest. Dermatol.*, **126**, 2377–2386.
17. Peters, T., Sedlmeier, R., Bussow, H., Runkel, F., Luers, G.H., Korthaus, D., Fuchs, H., Hrabe de Angelis, M., Stumm, G., Russ, A.P. *et al.* (2003) Alopecia in a novel mouse model RCO3 is caused by mK6irs1 deficiency. *J. Invest. Dermatol.*, **121**, 674–680.
18. Vielkind, U. and Hardy, M.H. (1996) Changing patterns of cell adhesion molecules during mouse pelage hair follicle development. 2. Follicle morphogenesis in the hair mutants, Tabby and downy. *Acta Anat. (Basel)*, **157**, 183–194.
19. Tumanov, A.V., Grivennikov, S.I., Shakhov, A.N., Rybtsov, S.A., Koroleva, E.P., Takeda, J., Nedospasov, S.A. and Kuprash, D.V. (2003) Dissecting the role of lymphotoxin in lymphoid organs by conditional targeting. *Immunol. Rev.*, **195**, 106–116.
20. Pruett, N.D., Tkatchenko, T.V., Jave-Suarez, L., Jacobs, D.F., Potter, C.S., Tkatchenko, A.V., Schweizer, J. and Awgulewitsch, A. (2004) Krtap16, characterization of a new hair keratin-associated protein (KAP) gene complex on mouse chromosome 16 and evidence for regulation by Hoxc13. *J. Biol. Chem.*, **279**, 51524–51533.
21. Rogers, M.A. and Schweizer, J. (2005) Human KAP genes, only the half of it? Extensive size polymorphisms in hair keratin-associated protein genes. *J. Invest. Dermatol.*, **124**, vii–ix.
22. Hardman, M.J., Moore, L., Ferguson, M.W. and Byrne, C. (1999) Barrier formation in the human fetus is patterned. *J. Invest. Dermatol.*, **113**, 1106–1113.
23. Cui, C.Y., Durmowicz, M., Ottolenghi, C., Hashimoto, T., Griggs, B., Srivastava, A.K. and Schlessinger, D. (2003) Inducible mEDA-A1 transgene mediates sebaceous gland hyperplasia and differential formation of two types of mouse hair follicles. *Hum. Mol. Genet.*, **12**, 2931–2940.
24. Cui, C.Y. and Schlessinger, D. (2006) EDA Signaling and Skin Appendage Development. *Cell Cycle*, **5**, 2477–2483.
25. Cui, C.Y., Durmowicz, M., Tanaka, T.S., Hartung, A.J., Tezuka, T., Hashimoto, K., Ko, M.S., Srivastava, A.K. and Schlessinger, D. (2002) EDA targets revealed by skin gene expression profiles of wild-type, Tabby and Tabby EDA-A1 transgenic mice. *Hum. Mol. Genet.*, **11**, 1763–1773.
26. Kere, J., Srivastava, A.K., Montonen, O., Zonana, J., Thomas, N., Ferguson, B., Munoz, F., Morgan, D., Clarke, A., Baybayan, P. *et al.* (1996) X-linked anhidrotic (hypohidrotic) ectodermal dysplasia is caused by mutation in a novel transmembrane protein. *Nat. Genet.*, **13**, 409–416.
27. Headon, D.J. and Overbeek, P.A. (1999) Involvement of a novel Tnf receptor homologue in hair follicle induction. *Nat. Genet.*, **22**, 370–374.
28. Headon, D.J., Emmal, S.A., Ferguson, B.M., Tucker, A.S., Justice, M.J., Sharpe, P.T., Zonana, J. and Overbeek, P.A. (2001) Gene defect in ectodermal dysplasia implicates a death domain adapter in development. *Nature*, **414**, 913–916.
29. Cui, C.Y., Smith, J.A., Schlessinger, D. and Chan, C.C. (2005) X-linked anhidrotic ectodermal dysplasia disruption yields a mouse model for ocular surface disease and resultant blindness. *Am. J. Pathol.*, **167**, 89–95.
30. Carter, M.G., Hamatani, T., Sharov, A.A., Carmack, C.E., Qian, Y., Aiba, K., Ko, N.T., Dudekula, D.B., Brzoska, P.M., Hwang, S.S. *et al.* (2003) *In situ*-synthesized novel microarray optimized for mouse stem cell and early developmental expression profiling. *Genome Res.*, **13**, 1011–1021.
31. Ware, C.F. (2005) Network communications: lymphotoxins, LIGHT, and TNF. *Annu. Rev. Immunol.*, **23**, 787–819.